ELASTIC-PLASTIC ANALYSES OF STRESS AND STRAIN FIELDS AROUND CRACK TIP

Wang Tzuchiang (王自强)
Institute of Mechanics, Academia Sinica, China

I. INTRODUCTION

Since Rice[1] proposed the J integral, much work has been published concerning single parameter to characterize the near crack tip behavior under large scale yielding conditions. Work of Hutchinson[2] and Rice and Rosengren[3] provided the theoretical basis for J integral criterion. It is important to determine the condition for J dominance of crack tip behavior. McMeeking and Parks[4] calculated the stresses and strains near the crack tip. They found that plots of stresses and strains versus $r/(J/\sigma_{ys})$ are independent of J for bend specimen. On the other hand, they found singnificant deviation from normalized S.S.Y. distribution for the center-cracked panel under large scale yielding condition. Work of Shih and German[5] has shown similar features. But the requirement that plots of stresses and strains versus $r/(J/\sigma_{ys})$ are independent of J is too restrictive for J dominated fields, because this requirement means that the stress and strain fields near crack tip are a continuous series of self-similar states and the size of dominated zone will proportionally increase with J integral. For example in order to get same value of $r/(J/\sigma_{ys})$ the distance r should increase 10 times when the J integral increases 10 times.

From a physical point view, fracture processes are only depending on the stresses and strains immediately near crack tip. Stresses and strains outside the fracture process zone are not important for fracture analysis.

This paper provides detailed analyses of the stress and strain fields around the crack tip in both hardening and nonhardening elastic-plastic materials. The stresses and strains at a fixed point immediately adjacent to the crack tip have been calculated for different geometry configurations and different sizes of specimens. The circumstances under which a single

parameter J can be used to characterize the crack tip fields have been discussed.

II. SOLUTION PROCEDURE OF PLANE-STRAIN CRACK PROBLEM

1) Variation Equation

The variation equation presented in [6] and [7] is

$$\delta U = \int_V F^{(1)} \cdot \tilde{V} dv + \int_{S_\sigma} P^{(1)} \cdot \tilde{V} \, ds \tag{1}$$

$$U = \frac{1}{2} \int_V \{ 2\mu [d_{ij} d_{ij} - \frac{\nu}{(1-\nu)} (d_{kk})^2 - \frac{\alpha}{g} (N_{ij} d_{ij})^2] - \sigma_{ij} (2 d_{ik} d_{jk} - V_{k,i} V_{k,j}) \} dv \tag{2}$$

Equation (1) is equivalent to the equilibrium equations of stress rate fields for large elastic-plastic deformation theory employing up-dated Lagrange coordinates. The finite element analyses are based on equation (1). The formulae of element stiffness matrix have been given in [7]. Eight-noded isoparametric element with 3 by 3 Gauss integration points are employed in the calculations for center cracked panel (CCP) and cracked bend bar specimen (CBB).

2) Finite Element Mesh

For long crack the finite element mesh employed is shown in Fig. 1 in its undeformed configuration. In zone C the 8 elements connected to the crack tip are degenerated to triangular elements. For hardening material, the crack tip nodes bond together and each triangular element has only six nodes. For nonhardening material, the degenerated elements still have 8 nodes and the two corner nodes and mid-side node are initially connected to the crack tip. As the load is increased, the crack-tip bluntting is modeled by the separating of nodes at the crack tip. The total mesh contains 432 nodes and 127 elements.

For short cracks, the finite element idealization used is the same as in [9]. The total mesh contains 398 nodes and 115 elements.

The smallest length of the crack tip elements is about 5—10% of the short crack length with ratio a/w = 0.024. The mesh is formed automatically

and can be easily changed.

For hardening material the true stress-strain curve is modelled by a power-law relationship of the form

$$\sigma_e = \sigma_{ys} (\bar{\varepsilon}_p / \bar{\varepsilon}_{po})^n \tag{3}$$

where σ_e is the equivalent stress, σ_{ys} is the yield stress, $\bar{\varepsilon}_p$ the equivalent plastic strain. The calculation uses an incremental tangent modulus procedure and contains approximately 200—300 load increments.

III. RESULTS OF LONG CRACK AND SHORT CRACK PROBLEMS

The calculations were carried out for plane strain and both a non-hardening and hardening material. Material properties were ν=0.3 and σ_{ys}/E=1/300.

For the power-law hardening material the hardening coefficient n was made equal to 0.1. The coefficient $\bar{\varepsilon}_{po}$ is equal to 0.002.

1) Stresses and Plastic Strains near Crack Tip for Hardening Material

In Fig. 2 the true stress σ_θ ahead of the crack tip is plotted against J integral. The J integral is normalized by $r_0 \sigma_{ys}$, where r_0 is the radial distance of a fixed point for which the stresses and strains are calculated. For cracked bend specimen (CBB), it is clear that the crack tip stress and strain fields are configuration-independent. The curves for both a/w=0.25 and a/w=0.75 are virtually identical for large scale yielding conditions and general yield conditions. On the other hand, for the center cracked panel(CCP) the stress and strain fields are a strong function of the geometry configuration and specimen size. When the specimen is large enough (i.e. r_o/w is small enough) the curve are close to that for CBB specimen under large scale yielding condition and general yielding condition.

According to the theory of dimensional analysis, the stress and strain fields only depend on nondimensional geometry parameters such as a/w, L/w etc. for the same material. For a given crack length a and specimen width w, one can imagine that there exists a small dominated zone in which r_0/w is small enough. Therefore for the center cracked panel, the dominated zone exists under large scall yielding and general yield condition, but the size of the dominated zone is quite small and will not proportionally increase with the increase of the J integral.

Especially when the crack is small, one can find significant deviation from that for CBB specimen even in the intermediate yielding range. The difference will increase with the increase of ratio r_0/w. Fig. 3 shows the equivalent plastic strain $\bar{\varepsilon}_p$ as a function of J integral. One can find that short crack exhibits an entirely different behavior from the long cracks. This is because the plastic zone develops rapidly and will surround the whole short crack under intermediate yielding range. Fig. 4 shows a typical plastic zone at two load levels K_1=11.7 $MNm^{-3/2}$ and K_1=13.7 $MNm^{-3/2}$. Therefore the local plastic flow is much easier than in the case of long cracks. This is the main reason why the plastic strain is much higher and the normal stress is much lower for short crack. The large specimen with short crack also exhibits a different behavior with that for long cracks.

2) Stress and Strains near Crack Tip for Nonhardening Material

As pointed by McClintock[8], the slip line fields near the crack tip for the center cracked panel are entirely different from that for bend specimen. The hydrostatic stress level near the crack tip is much lower than the level in the bend specimen. Therefore the crack tip fields under general yielding condition should be configuration-dependent.

Fig. 5 shows the normal stress σ_θ as a function of J integral. For small scale yielding and long crack the normal stress will increase with increase of the J integral and the crack tip fields seem configuration-independent. Especially for bend specimen the crack tip fields are really independent of ratio a/w even under general yielding condition.

From a macromechanics viewpoint one can imagine that the zone between a blunted crack tip and intersect of two logarithmic spiral lines as shown in the inset of Fig. 5 is the intense strain zone. According to the perfect plasticity theory, the size of the intense strain zone r_e, is approximately equal to 2.405 δ=2.405 J/σ_{ys}. When the value $J/(r_0\sigma_{ys})$ is equal to 1/2.405, i.e. when the intense strain zone size reaches r_0, the crack tip fields display some differences for different geometries. The normal stress reaches a maximum value of 3.10 σ_{ys} and approximately equals the value 2.97 σ_{ys} in Prandtl's slip line field solution for bend specimen.

For center cracked panel, the maximum value of ($\sigma_{\theta max}$) is a little bit lower than 2.97 σ_{ys}. After reaching the maximum value ($\sigma_{\theta max}$), the normal stress σ_θ will decrease with increase of the J integral and show

significant deferences for different geometries. Fig. 5 also shows the normal stress σ_θ for the center cracked panel with a short crack. It is clear that the stress σ_θ deviates sharply from that for the bend specimen results even under small scall yielding conditions.

Fig. 6 shows the equivalent plastic strain $\bar{\varepsilon}_p$ as a function of J integral. One can conclude that the crack tip fields are dominated by J integral for bend specimens, but the crack tip fields can not be characterized by the J integral for the center cracked panel.

IV. CONCLUSIONS

From the numerical results one can draw several tentative conclusions:

1) For the bend specimen with long crack the crack tip fields are configuration-independent and can be characterized by the J integral even for the nonhardening material.

2) For the center cracked panel and hardening material with long crack, there exists a dominated zone in which the stress and strain fields can be approximately characterized by the J integral, but the dominated zone size is quite small and will not increase in proportion with the increase of J integral.

3) Short crack exhibits entirely different crack tip stress and strain fields. For the same value of J integral, the stress level is much lower than that for long cracks and the plastic strains are much higher than that for long cracks if the nonhardening or low strain hardening material is concerned.

ACKNOWLEDGMENT

The author wishes to thank Professor K.J. Miller (Department of Mechanical Engineering, Sheffield University) for his encouragement. Many helpful discussions with Dr. E. Hay are gratefully acknowledged.

REFERENCES

[1] Rice, J.R., Journal of Applied Mechanics, Vol. 35(1968), 379–386.

[2] Hutchinson, J.W., Journal of the Mechanics and Physics of Solids, Vol. 16(1968), 13–31.

[3] Rice, J.R. and Rosengren, G.F., Journal of the Mechanics and Physics

of Solids, Vol. 16(1968), 1–12.

[4] McMeeking, R.M. and Parks, D.M., ASTM STP 668 (1980), 175–194.

[5] Shih, C.F. and German, M.D., Inter. Joun. of Fracture, 17 (1981), 27–43.

[6] McMeeking, R.M. and Rice, J.R., Int. J. Solids Struct., Vol. 11 (1975), 601–616.

[7] Wang, T.C., Acta Mechanica Sinica, Special issue (1980), 182–192.

[8] McClintock, F.A., in "Fracture: An Advanced Treatise, H. Libowitz, Ed. Vol.3, Academic Press, New York (1971), 47–225.

[9] Wang, T.C. and Miller, K.J., Journal of Fatigue of Engineering Materials and Structures, Vol.5 (1982), 249–263.

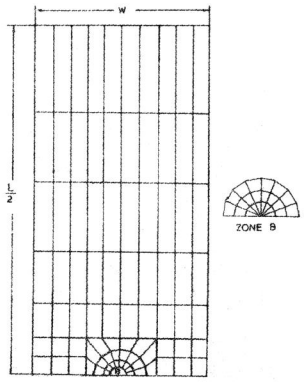

Fig.1 Finite element mesh for long cracks

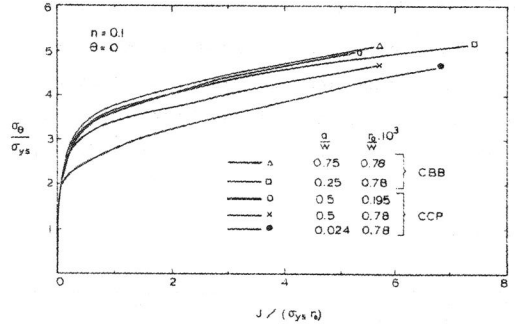

Fig.2 Stress ratio $\sigma_\theta/\sigma_{ys}$ vs $J/(\sigma_{ys}r_0)$ at θ=0 for a hardening material

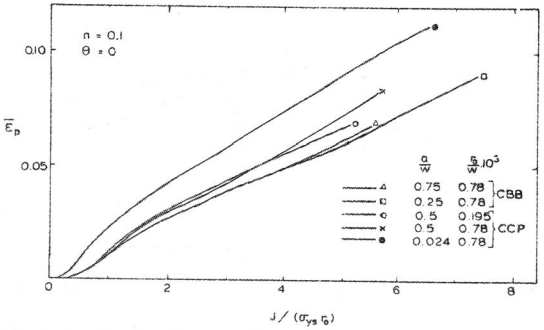

Fig.3 Equivalent plastic strain ahead of a crack tip as a function J integral for a hardening material.

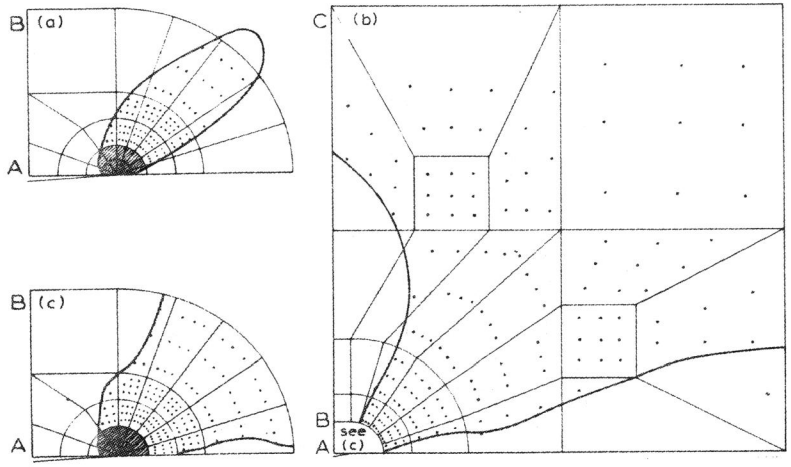

Fig.4 Plastic zone shapes for a CCP specimen and a hardening meterial (n=0.2). Note the hatched area is plastically deformed but too small to show the integration points. Here W=20 mm, a=0.1 mm. (a) K_I=11.7 $MNm^{-3/2}$, (b) K_I=13.7 $MNm^{-3/2}$. (c) Enlargement of (b) near the tip

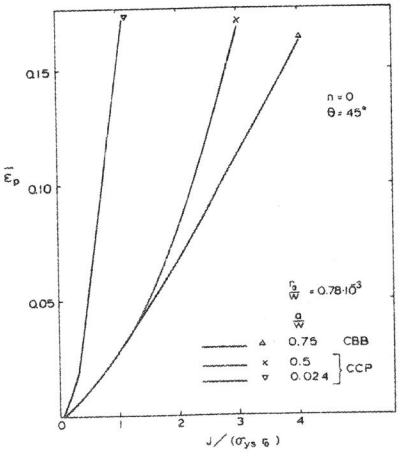

Fig.5 Stress ratio $\sigma_\theta/\sigma_{ys}$ vs $J/(\sigma_{ys}r_0)$ for a non-hardening material

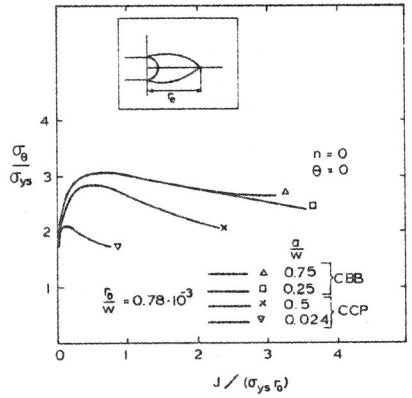

Fig.6 Equivalent plastic strain vs $J/(\sigma_{ys}r_0)$ for a non-hardening material

ON INCLINED CRACK UNDER COMPRESSIVE LOADING

C.W. Woo & C.L. Chow
University of Hong Kong
Department of Mechanical Engineering

ABSTRACT

The effect of compressive loading on an inclined crack is examined in this investigation. Four fracture criteria, namely the maximum hoop stress, the strain energy density, the potential energy release rate, and the energy-momentum tensor, are reviewed. A modified model is proposed to include the frictional effect of the sliding mode under compressive loading. The predictions of the initial direction of crack growth are compared to experimental results over a wide range of inclined crack angles.

INTRODUCTION

The inclined crack problem under mixed mode loading has been a controversial topic in recent literature in fracture mechanics. A popular representation of a two-dimensional mixed mode loading case is a straight crack oriented at an angle β to the uniaxial tension (Figs. 1 & 2). When $\beta = 90^0$, the classical Griffiths crack is resumed and once the critical fracture load is reached, the crack will start to propagate in the direction of its own plane. For values of β other than 90^0, similarity is lost in that propagation starts with crack initiation angle θ_0 different from zero. The problem involves the prediction of initial crack growth angle θ_0 and the magnitude of the applied load σ_{cr} at which growth occurs.

In an early attempt to solve this problem Erdogan and Sih [1], Ewing and William [2, 3] made use of the maximum hoop stress at the crack tip as a criterion. Later Sih [4, 5, 6] proposed a new concept using the strain energy density criterion. Extension of the original Griffith's fracture criterion to the inclined crack problem was pursued by several reseachers [8, 9, 10, 11] using potential energy release rate G. Another alternative approach was proposed by Tirosh [12] using Eshelby's energy-Momentum tensor [13].